ERDC TN-DOER-E30
January 2012

Ground Truth Sampling to Support Remote Sensing Research and Development: Submersed Aquatic Vegetation Species Discrimination Using an Airborne Hyperspectral/Lidar System

by *Molly Reif [1], Candice Piercy [2], Jessie Jarvis [3], Bruce Sabol [2], Chris Macon [4], Richard Loyd [5], Phil Colarusso [6], Heidi Dierssen [7], and Jen Aitken [8]*

INTRODUCTION: Inferring conditions about the earth's surface using remotely sensed electro-optical measurements almost always requires the use of reference, or "ground truth" data. Ground-based measurements typically involve collecting measurements of the phenomena or target being remotely sensed and can range from employing physical field checks to aerial photography (Lillesand et al. 2004). More commonly, they include physical and chemical measurements with geographic positions and observations for comparison with remotely sensed imagery. Generally, ground truth is used to assist with 1) image analysis and interpretation (e.g. image classification) of remotely sensed imagery, 2) remote sensor calibration, and 3) accuracy assessment of image analysis results (Lillesand et al. 2004).

Much of the emphasis on collecting ground truth is for verification and assessment of imagery analysis; however, there are no universally accepted standards for assessing accuracy (Congalton and Green 2009). Considerations for assessing accuracy in the collection of ground truth should include such topics as the distribution of the phenomena being mapped, sample size, number, type, and frequency of collection, and consistency and objectivity in measurement and collection (Congalton and Green 2009). Researchers in the 1970s began to introduce simple techniques for accuracy assessment (Ginevan 1979), followed by more detailed efforts described in Congalton et al. (1983). Furthermore, some guidance and examples for statistically sound approaches in determining sample size are available (Hord and Brooner 1976, van Genderen and Lock 1977, Hay 1979, Rosenfield et al. 1982, Congalton 1988). Also, consideration for choosing the appropriate sampling strategy is described in Ginevan (1979), Fitzpatrick-Lins (1981), and Stehman (1992).

When a remote sensing or image processing technique is under development, it is mandatory to have sufficient ground truth data to test not only the accuracy of the final image analysis output, but also the intermediate steps in that process. General guidance for ground truth collection in

[1] U.S. Army Engineer Research and Development Center, Joint Airborne Lidar Bathymetry Technical Center of eXpertise, Kiln, MS
[2] U.S. Army Engineer Research and Development Center, Vicksburg, MS
[3] Biology Department, Richard Stockton College, Pomona, NJ
[4] U.S. Army Corps of Engineers, Mobile District, Joint Airborne Lidar Bathymetry Technical Center of eXpertise, Kiln, MS
[5] U.S. Army Corps of Engineers, New England District, Concord, MA
[6] U.S. Environmental Protection Agency, Boston, MA
[7] Dept. of Marine Sciences, University of Connecticut, Groton, CT
[8] Optech International, Kiln, MS

remote sensing research and development (R&D) is extremely limited, as it is dependent on specifics of the technology being developed. Although much work has been done to develop procedures for accuracy assessment, there is a need to better understand and develop the role of ground truth and collection methods for evolving remote sensing technology.

BACKGROUND: Submersed aquatic vegetation (SAV) is an important indicator of environmental quality (Dennison et al. 1993, Moore 2004) and provides a variety of ecological benefits, including the prevention of coastal erosion (Fonseca and Cahalan 1992) and the provision of fisheries habitat (Duffy and Baltz 1998, Richardson et al. 1998). However, populations of SAV are declining globally (Orth et al. 2006), primarily as a result of reduced water clarity (Dennison et al. 1993, Tamaki et al. 2002, Kemp et al. 2005), some of which may be attributable to effects of dredging and sand mining (Orth et al. 2006). The Clean Water Act (CWA) Section 404(b)(1) guidelines list SAV beds as Special Aquatic Sites, requiring the U.S. Army Corps of Engineers (USACE) to avoid or minimize habitat impacts and to compensate for habitat loss when impacts cannot be avoided. SAV tends to be more prevalent in protected embayments, which are also favored for locating boating infrastructure, such as marinas, mooring fields, navigation channels, piers, and docks. Consequently, when planning dredging operations it is necessary to map SAV distribution and to distinguish between ecologically valuable species subject to CWA protection and less important species such as marine macroalgae.

Most SAV mapping studies have utilized aerial photography (McKenzie et al. 2001, Costello and Kenworthy 2011) and multispectral imagery to identify the areal coverage and density of seagrass beds. While these technologies can be effective in detecting SAV, they do not reliably distinguish between species of SAV. Alternative methods, such as acoustic mapping and videography, provide a finer level of detail, although they are limited in areal coverage (Sabol et al. 2002, Sprenkle et al. 2004). Newer remote sensing techniques have emerged to provide innovative approaches for improved accuracy and capabilities. Spaceborne sensors, such as IKONOS, Quickbird, Landsat 7, SPOT 5, and ASTER, provide a range of improved remote sensing properties, including such advantages as higher spatial and spectral resolutions, higher temporal frequency, and larger geographic extent (Dekker et al. 2006). Recent studies have utilized multispectral remote sensing to map SAV characteristics, including distribution and density (Wang et al. 2007, Wolter et al. 2005, Yuan and Zhang 2008). In addition, studies utilizing hyperspectral imagery have resulted in improvements to distinguish SAV species (Phinn et al. 2008, Pinnel et al. 2004, Thorhaug et al. 2007, Williams et al. 2003).

One of the main challenges in using remote sensing to classify bottom conditions is the spectral/optical effect of the water column on the spectral signature of the benthic material. Through processes of absorption and scattering, light is altered by water and optically active constituents, modifying the target signal of interest (Silva et al. 2008, Zimmerman and Dekker 2006). It is this signal that must be separated from the interference and optical properties of the water column, which can vary greatly due to wind, wave, tide, and other environmental conditions. Aside from light attenuation in the water column, other related challenges with mapping SAV include generally low reflectance signals, and overlapping spectral reflectance properties of various benthic surfaces. These combined factors make detection and species discrimination of SAV much more challenging than similar tasks for terrestrial vegetation (Dekker et al. 2006), and strengthen the need for detailed ground truth data. In response to these

challenges, remote sensing techniques for overcoming them are continually being developed and improved. In hyperspectral image processing, radiometric corrections can be conducted, removing atmospheric, air-water interface, and sun-angle effects to obtain the reflectance component coming from the water column and seafloor, referred to as water-leaving reflectance. Processing techniques can reveal information on water depth, water column constituents, and ultimately, the benthic reflectance properties (Aitken et al. 2010, Silva et al. 2008, Zimmerman and Dekker 2006). The resultant inverted image and corrected benthic reflectance can then be analyzed and classified into various types or species based on their unique spectral characteristics. Studies employing such techniques coupled with detailed ground truth data have shown encouraging results in discriminating benthic cover types, including areas with SAV (Brando and Dekker 2003, Phinn et al. 2008).

This remote sensing R&D effort seeks to demonstrate the value of fusing depth data, generated from bathymetric lidar, with hyperspectral reflectance data to detect and discriminate SAV species and map benthic conditions. Sensor data for this effort are collected by an integrated airborne sensor suite described below. Developing and demonstrating this technique requires extensive ground truth data, described in this document. The objectives of this work are to: 1) develop and test image fusion techniques, 2) compare them to more traditional techniques, and 3) determine the appropriate level of technology for this detection/discrimination task.

PURPOSE: This technical note documents a multifaceted ground truth data collection effort to support R&D of an aquatic remote sensing application. The data collected have utility for a variety of purposes and researchers beyond this R&D project. The scope of this document is to describe the ground truth sampling design and its development, the component data types and their uses, and the database used to store and manage the data. The results of the remote sensing study will be summarized in a separate manuscript generated at the end of this project. That manuscript will also contain a critical evaluation of the effectiveness of this ground truth sampling effort.

SYSTEM COMPONENTS AND DATA: The system used to acquire the lidar bathymetric data and hyperspectral imagery for this study is the Compact Hydrographic Airborne Rapid Total Survey (CHARTS). CHARTS is jointly operated and maintained by the USACE and the U.S. Naval Oceanographic Office (NAVO). It features an Optech Inc. SHOALS-1000, with a 1-kHz bathymetric lidar (full waveform, 7-nanosecond [ns] pulse) and a 9-kHz topographic lidar (discrete return), an ITRES Compact Airborne Spectrographic Imager (CASI)-1500 for hyperspectral imaging, and a DuncanTech-4000 3-band RGB digital camera (Wozencraft and Lillycrop 2006). From this integrated, airborne sensor suite (Figure 1), topographic and bathymetric lidar and aerial and hyperspectral imagery are

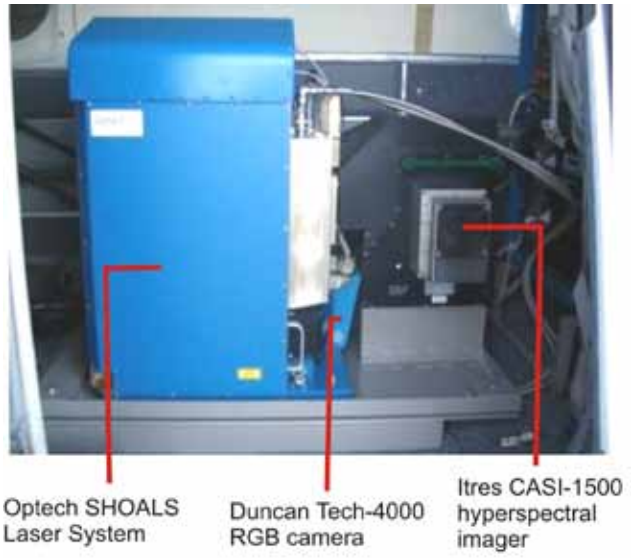

Figure 1. CHARTS system aboard the aircraft.

further processed into an assortment of Geographic Information Systems (GIS) data products for the National Coastal Mapping Program (NCMP), executed by the Joint Airborne Lidar Bathymetry Technical Center of eXpertise (JALBTCX). This study utilizes data products generated from this survey, including 1-m hyperspectral image data geometrically and atmospherically corrected with 36 spectral bands at 18 nanometer (nm) bandwidth in the 380- to 1050-nm spectral range, bathymetric lidar collected with a 4-m spot spacing (± 30-cm vertical accuracy), collecting values in the 532-nm wavelength, and 20-cm RGB aerial image mosaics.

SITE DESCRIPTION: In 2010, the NCMP surveyed coastal areas between Cape Canaveral, Florida and Maine. Prior to the survey, coordination meetings were held with the USACE coastal districts within this area to identify specific coastal areas with coastal engineering or environmental issues that could be addressed with CHARTS data. Because of previous work with the New England District (NAE), issues of mapping SAV and distinguishing eelgrass (*Zostera marina*) from other co-occurring marine macroalgae species in shallow water dredging sites were known (Sabol et al. 2005, 2008). Demonstration sites within NAE were selected based on: 1) occurrence of multiple species of SAV and/or macroalgae, 2) upcoming maintenance of dredging activities, and 3) logistical ease. As a result, two southeastern Massachusetts harbors were identified: Plymouth Harbor and Buttermilk Bay Entrance Channel, MA.

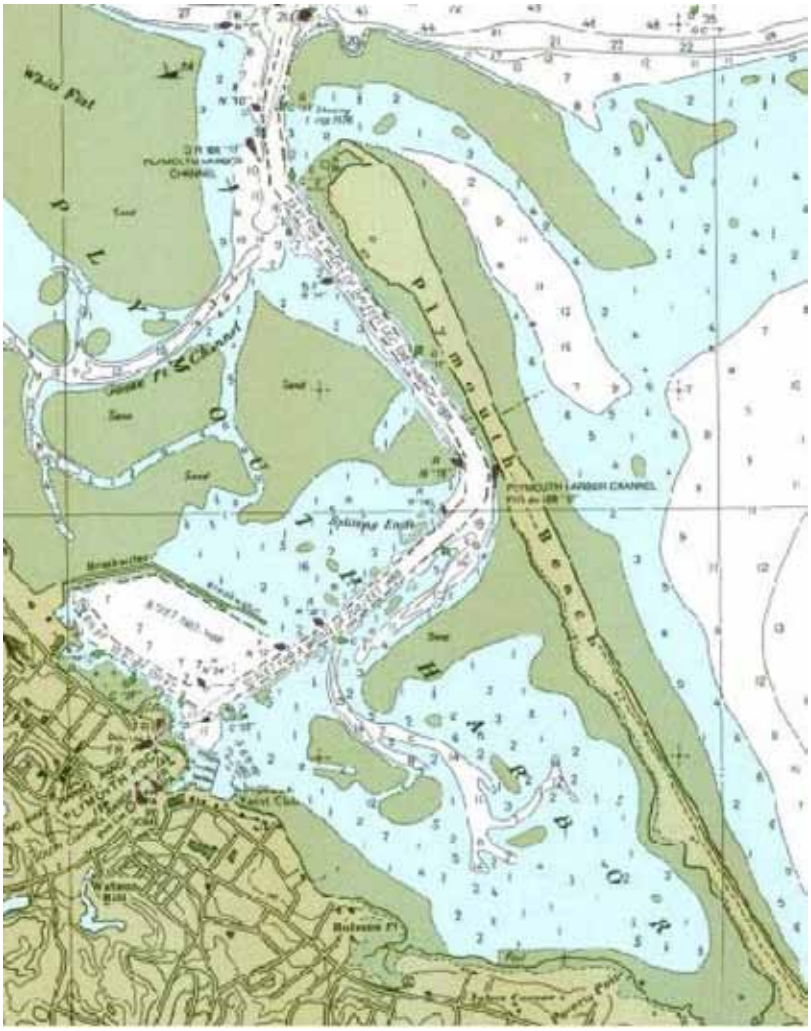

Figure 2. Federal Navigation Channel in Plymouth Harbor, MA.

Plymouth Harbor. Plymouth Harbor is located on the south shore of Massachusetts, in the town of Plymouth (Figure 2). The harbor contains a working town wharf for commercial fishermen, a yacht club, a significant recreational fleet, public facilities, and harbor-side historical attractions. The harbor contains a Federal navigation project consisting of a 200-ft-wide main entrance channel that is authorized to be maintained at 18 ft (5.5 m) deep at Mean Lower Low Water (MLLW), a150-ft-wide and 15-ft-deep (4.6 m) channel extension and turning basin, and a 60-acre by 8-ft- (2.4-m-) deep anchorage (USACE, New England District 2005). The 18-ft-deep channel is approximately 2.5 miles (4 km) long and the 15-ft

channel is about 0.3 mile (0.48 km) in length. The tidal range in Plymouth Harbor is approximately 9 ft. Several small freshwater discharges into the surveyed area (see Mission Planning section) do not generally affect water clarity in the harbor throughout the tidal cycle.[1]

Buzzard's Bay. For the purposes of this document, the area surveyed in the Buzzard's Bay region will be referred to as the Buttermilk Bay Entrance Channel. This site is a federal navigation project that includes a 7-ft-deep, 100-ft-wide channel at MLLW through the sandbar blocking the natural channel, connecting Buzzard's and Buttermilk Bays. The channel extends about 2,800 ft from the west side of the Cape Cod Canal in the vicinity of Sears Point, Wareham, first northwesterly and northeasterly to a point midway between Taylor Point, Bourne, and Peters Neck, Wareham, about 2,800 ft southwest of the entrance to Buttermilk Bay. Additional authorization extended the channel 2,500 ft, 6 ft deep and 80 ft wide to the site of a public marina (Taylor Marina). The project was completed and last maintained in 1984. Tides within Buzzard's Bay typically range around 4 ft and water clarity within the area changes significantly over the tidal cycle due to turbid waters entering from a tributary at the north end of the project.[1]

Figure 3. Federal Navigation Channel in Buttermilk Bay Entrance

MISSION PLANNING: Planning the CHARTS survey mission and selecting candidate mission survey windows is a multiple-constraint problem. It is either mandatory or highly desirable that various factors be within a specific range of values, otherwise the resulting imagery will not meet mission objectives. Overall mission objectives are to get a simultaneous set of co-registered bathymetric lidar data and hyperspectral imagery over each harbor under optimal conditions to

[1] Personal communication, 2010.William Hubbard, Evaluation Branch Chief, U.S. Army Engineer District, New England.

detect and discriminate species of SAV and macroalgae, while also testing the image-processing algorithms used for detection and discrimination. Conditions evaluated in planning these missions are listed in Table 1.

Table 1. Mission planning factors.

Factor	Level/condition	Criticality	Notes
GPS PDOP[1]	<3.0	Mandatory	Required for image geo-rectification
Solar Elevation	>30 degrees and <50 degrees above horizon	Mandatory	Required for hyperspectral data
Flightline Orientation	Into/out of sun; away from sun is preferable	Highly desirable	Required to minimize solar glint
Cloud Cover	<10%	Mandatory	Required for hyperspectral data
Sea State	Minimal white capping	Highly desirable	
Tide	Above mean and rising or high	Highly desirable	Required for water clarity and coverage of shallow flats
Wind	<30 knots	Mandatory	Required for flight safety; less white capping

[1] PDOP = Position Dilution of Precision

Factors such as GPS PDOP, sun angle, and tides are predicted in advance for identification of potential survey window dates and times. The mission planning is used to assist with mobilization of crew and equipment to the field at the appropriate date and time and overall preparation for the survey mission, subject to factors that are not known far in advance such as weather. For the primary flight window, 15-17 September 2010, mission planning graphics are illustrated for both study sites (Figure 4). Mission planning analyses were performed by Chris Macon of JALBTCX.

Based on these factors, primary and secondary survey windows were identified (Figure 4: blue is optimal (primary) survey window, with all factors satisfied and yellow is a secondary choice survey window, with some factors satisfied). As a result of the analysis, Plymouth Harbor revealed an optimal flight window with tides above mean sea level, sun azimuth >140, sun elevation >30, and PDOP <3. These conditions were optimal during the morning hours (approximately 8 am to 10 am between 16 September and 17 September). In contrast, Buttermilk Bay Entrance Channel revealed an optimal survey window with tides above mean sea level, sun azimuth >200, sun elevation >30, and PDOP <3. These conditions were optimal in the early afternoon hours (approximately 1 pm to 3 pm between 15 September and 17 September). Given these times and associated solar azimuths, the flightlines were planned such that the sun was at the nose or tail of the plane (Figures 5 and 6). This orientation comes close to equalizing the viewing angle (angle between sensor and sun) across all flightlines for the passive sensor, and minimizing solar glint, which is detrimental to image quality. Spacing of the flightlines gives a sidelap (overlap between adjoining flightlines) of approximately 25 percent.

The CASI sensor has the most restrictive set of conditions needed for high quality imagery, while good bathymetric lidar data can be acquired under a wider range of conditions. Weather is

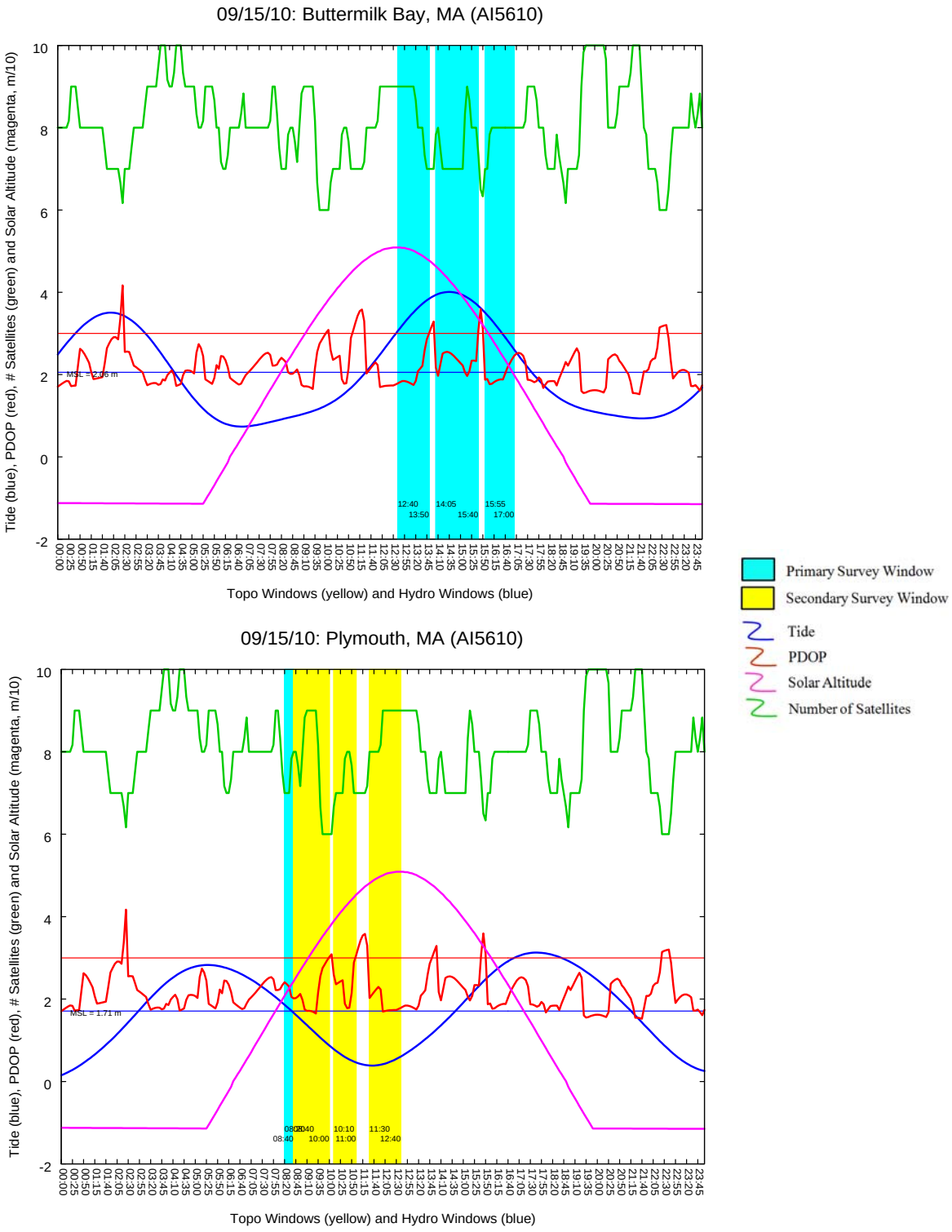

Figure 4. Flight window planning for Plymouth Harbor and Buttermilk Bay Entrance Channel, MA (Sheet 1 of 3).

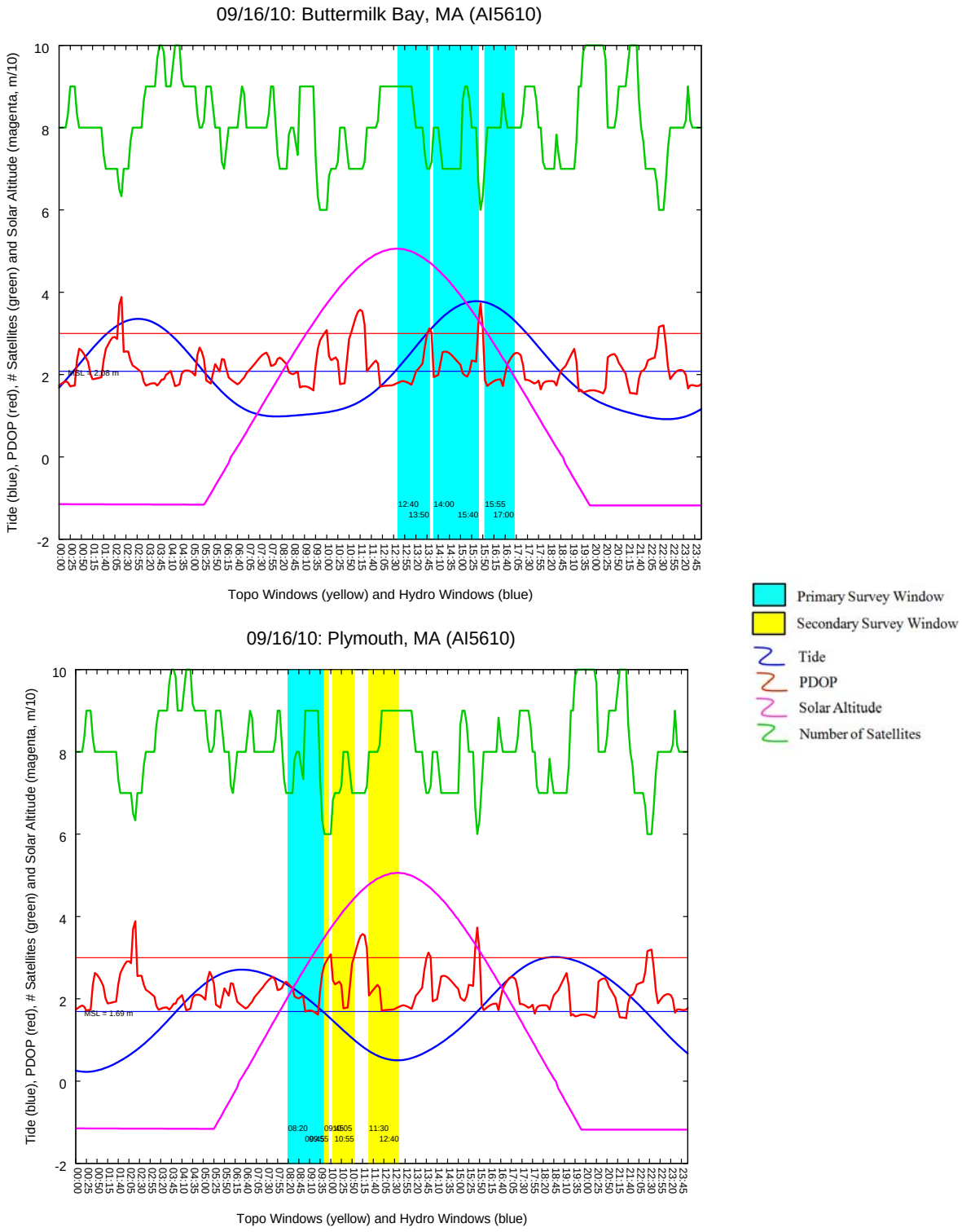

Figure 4. (Sheet 2 of 3).

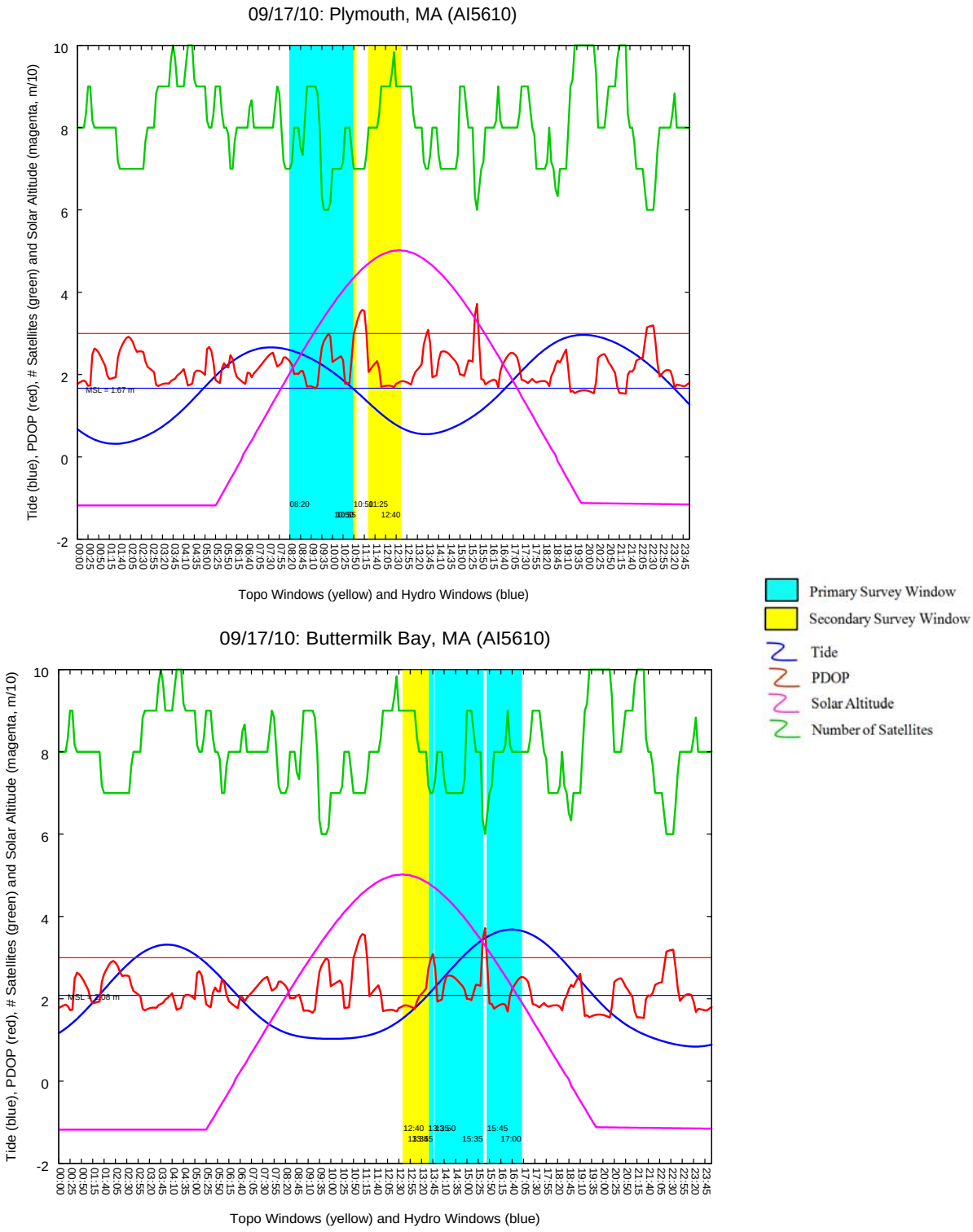

Figure 4. (Sheet 3 of 3).

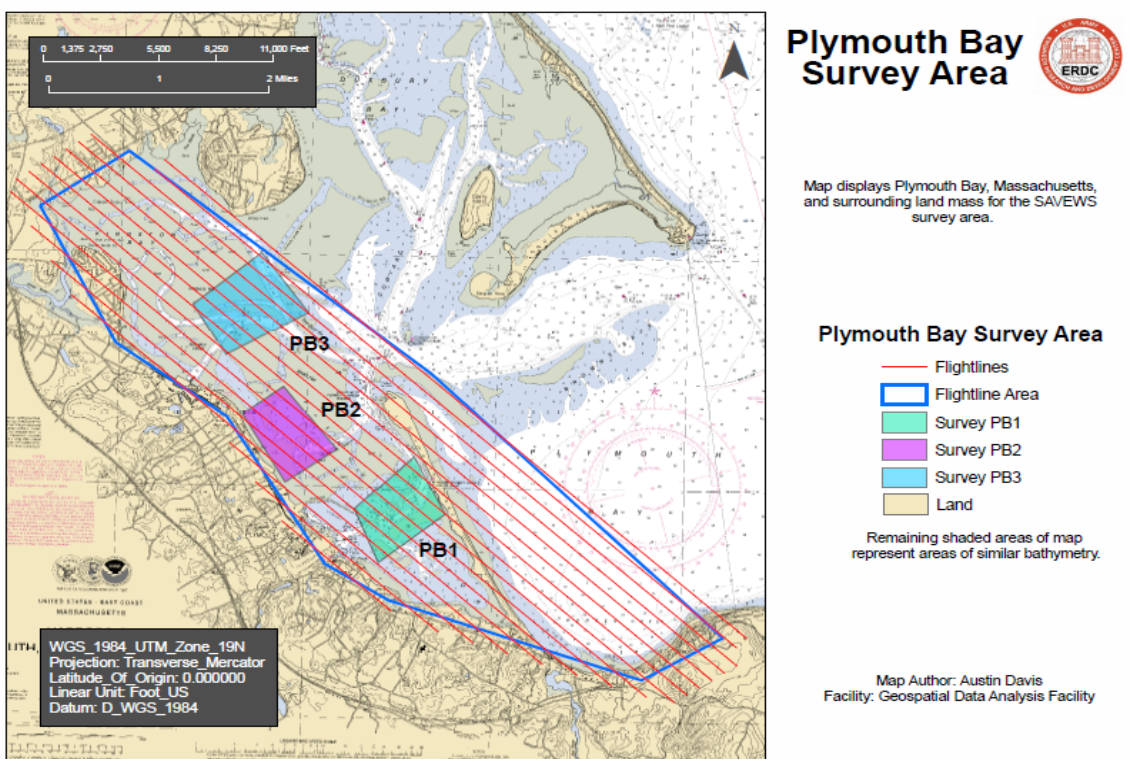

Figure 5. Map of Plymouth Bay (Harbor) survey site. Red lines denote flight lines for airborne sensors. Shaded areas denote areas for acoustic and spectral surveys.

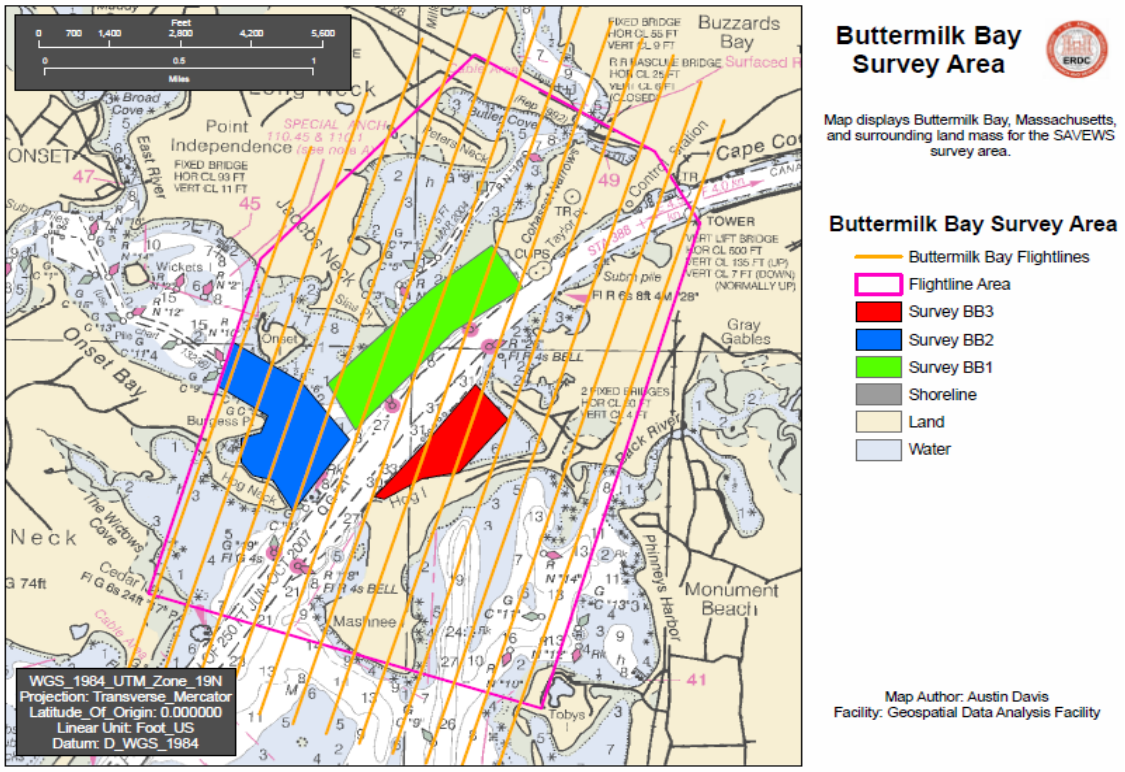

Figure 6. Map of Buttermilk Bay survey site. Red lines denote flight lines for airborne sensors. Shaded areas denote areas for acoustic and spectral surveys.

the least predictable condition and controls cloud cover, wind, and sea state. Minimal cloud cover is critical for the CASI imagery and proved to be the most difficult condition to satisfy. During the primary imaging time, the weather was generally clear in the morning with cloud cover increasing in the afternoon. Accordingly, missions at both sites were flown on 15 and 16 September. Between the double imagery sets, excellent imagery was obtained for 95+ % of each site.

GROUND TRUTH DATA COLLECTION: The overall components of this research and their sequencing are illustrated in Figure 7. Initial mission planning began in January 2010 with the identification of the two study sites. Selection of mid-September for the overflight was based on the need for SAV to be near peak biomass, before the onset of SAV dieback and the onset of fall storms with associated higher turbidity and cloud cover. The flightline areas (Figures 5 and 6) were selected by the NAE based on their project interests and information indicating multiple species of SAV. Preliminary mission analyses (Figure 4) roughly determined the time of day of the overflight and the solar azimuth during this period, which established the orientation of the flightlines. During a preliminary site visit in July 2010, SAV and sediment samples were collected for laboratory hyperspectral reflectivity measurement using an ASD FieldSpec Pro. Based on these measurements, the configuration of the CASI-1500 was programmed to collect 36 spectral bands with the 18-nm bandwidth in the 380- to 1050-nm spectral range.

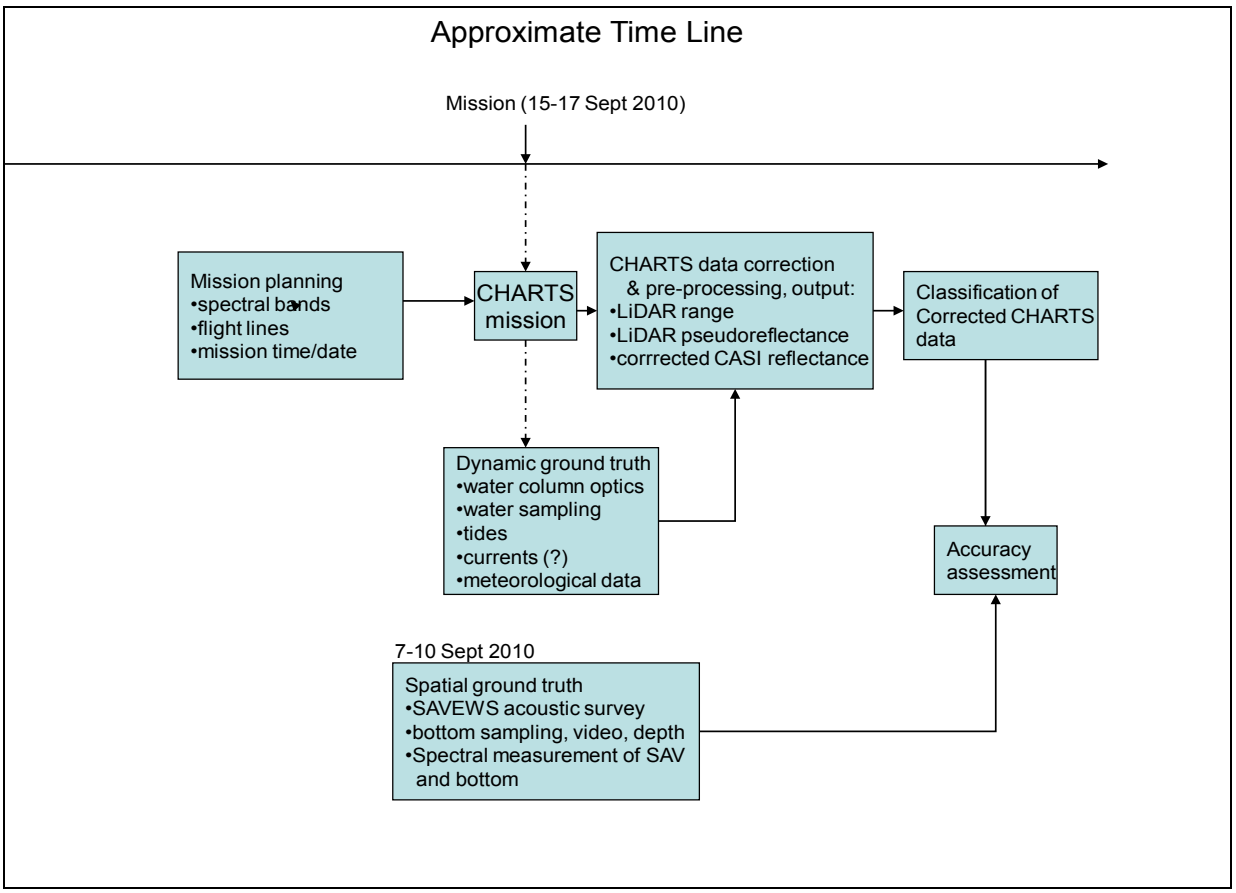

Figure 7. Components of overall study.

Ground truth sampling efforts were divided into two distinct components – spatial and dynamic (Figure 7). The spatial ground truth refers to measurement of scene properties that are not likely to change within a few weeks of the overflight mission. They consist of location-referenced observation, in situ measurements, and physical sampling of SAV and bottom sediments. Spatial ground truth efforts were initiated with acoustic surveys conducted on 7 September at Plymouth Harbor and on 8 September at Buttermilk Bay Entrance Channel (see Acoustic Survey section). These surveys were performed within three regions at each site (Figures 5 and 6) to detect and map the SAV canopy geometry (depth, SAV coverage, and SAV canopy height) along linear transects in each region. These data provide a good indication of SAV presence and relative height/density but not species composition. These data provided the most current information on SAV presence within these regions and are used to select sampling locations for other spatial ground truth sampling.

Specific points selected from this acoustic sampling data set were used for other spatial ground truth sampling, including: in situ hyperspectral measurements of SAV and sediments performed by diver-operated DiveSpec (see "In Situ Underwater Hyperpsectral Reflectance Measurement" section), underwater video imagery collected by a drop camera (see "Underwater Video Drop Camera" section), and diver observation and sampling of SAV by the Environmental Protection Agency (EPA) Dive Team (see "Diver Sampling" section). Additionally, a ground-based team conducted in situ hyperspectral measurements of onshore and shallow water features using the ASD FieldSpec Pro (see "In Situ Shoreline and Shallow Water Hyperspectral Reflectance Measurement" section). The number of sampling points for each data type was determined based on available time and budget, and not by any statistical analyses; the consequences of this practical limitation will be evaluated in the final manuscript. The overall sampling design and schedule were developed by Dr. Jessie Jarvis and are contained in Appendix A.

The components of the spatial ground truth sampling served several purposes. All components provide data that can be used in the accuracy assessment of final image classification results. The output classification generated from the image classifier is compared with measurements and observations made at these points, thus determining the accuracy of the classifier. In situ hyperspectral measurements made underwater with the DiveSpec and on land with the ASD FieldSpec will be used to evaluate spectral separability of the various surface and subsurface types. In addition, the data will be used to assist with classification algorithm selection and evaluate advanced inversion calculations to eliminate atmospheric and water column effects from raw CHARTS data to predict true reflectance of each surface.

Dynamic ground truth sampling consists of variables that must be measured at the exact time of the overflight mission since they can change rapidly. These measurements include spectral irradiance (see "Spectral Irradiance" section), tidal height (see "Tide Measurement" section), and water column optical properties and chlorophyll sampling (see "Water Column Optical Measurements" section). Tide data are used to validate predicted tidal conditions for the survey mission and can be useful for image interpretation. Spectral irradiance, water column optical properties, and chlorophyll measurements serve as parameter inputs within the preprocessing of CHARTS data to remove atmospheric and water column effects.

TECHNICAL DESCRIPTION OF GROUND TRUTH MEASUREMENTS: Procedures used for each ground truth data component are described in this section and examples of each data type are presented. Each measurement type was conducted in accordance with the highly detailed field sampling plan contained in Appendix A.

Acoustic survey. The acoustic survey was conducted with the ERDC-developed Submersed Aquatic Vegetation Early Warning System (SAVEWS; Sabol et al. 2002, 2009) from aboard an NAE survey boat equipped with GPS navigation capability. SAVEWS is operated by running parallel linear transects using a narrow-beam, high-frequency, vertically aimed echosounder transducer linked with a high accuracy real-time differentially corrected GPS. The recorded data stream is post-processed to generate a stream of position-referenced attributes including depth, SAV coverage, and SAV canopy mean height at an output rate of 1 Hz. These data are further processed to a user-selected horizontal coordinate system with vertical depth correction for tides and transducer depth. Acoustically determined SAV canopy height is not considered a reliable estimate of true canopy height because surveys were conducted during periods of high tidal flow, during which the plants were lain over. Therefore canopy height data should be interpreted as the lower range of in situ canopy height. Acoustical analyses were conducted by Bruce Sabol of ERDC.

The three regions selected within each site (Figures 5 and 6) were picked based on boat accessibility during all tide stages and on known occurrence of SAV in these regions. Approximately 25 pre-planned parallel transects, spaced at approximately 40 m, were programmed into the survey boat's GPS for each region at each site. During acoustic sampling it became apparent that time would not allow for sampling all intended transects; therefore, the transect spacing was increased to approximately 100 m to complete the task in the available time. SAV coverage for each survey is illustrated (Figure 8). Based on these results, points were selected for other spatial ground truth sampling components to provide a range of SAV conditions.

In Situ underwater hyperpsectral reflectance measurement. The DiveSpec is a submersible underwater reflectance and fluorescence spectroradiometer manufactured by NightSea LLC of Andover, Massachusetts with operational support for this acquisition provided by Optech International (Figure 9). It is designed to collect three kinds of measurements: reflectance, radiance, and fluorescence in the spectral range of 400 to 750 nm. Reflectance (technically Remote Sensing Reflectance) is expressed here as:

$$L_u / E_d$$

where:

L_u = upwelling radiance from test surface
E_d = incoming solar irradiance

Reflectance of a surface can be measured with the DiveSpec in two ways: either by using incoming solar illumination or instrument-generated illumination. The DiveSpec is unique in that it can generate its own white light source in the measurement probe, thus eliminating reliance on incoming solar irradiance (E_d) and allowing spectral measurements to be collected free of

a) Plymouth Harbor

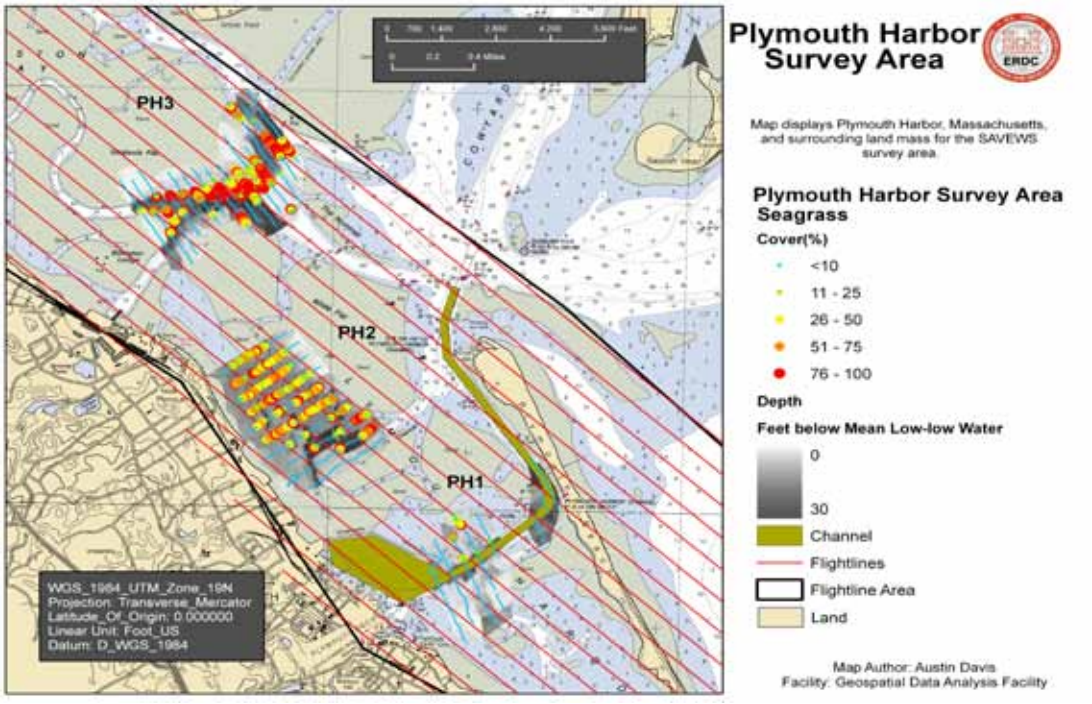

b) Buttermilk Bay Entrance Channel

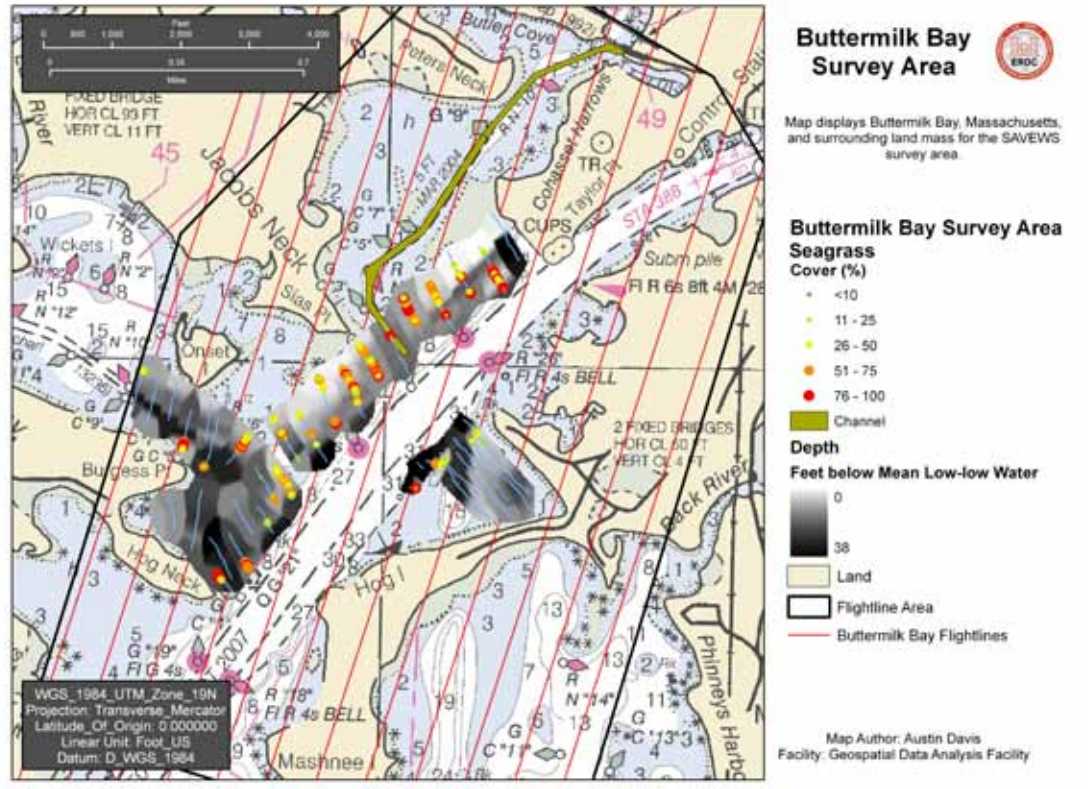

Figure 8. SAV coverage estimated by acoustic survey, a) Plymouth Harbor, b) Buttermilk Bay Entrance Channel.

variable cloudiness, wave focusing, self-shadowing, and other effects. In both methods a white panel of known calibrated reflectance is measured first to obtain E_d, then the surface is measured to obtain L_u. Radiance is measured by holding the DiveSpec instrument probe above a surface that is illuminated by incoming solar irradiance, much the same way radiance is measured with traditional handheld spectrometers. The probe does not generate its own light in this mode.

Figure 9. DiveSpec instrument.

The DiveSpec was used to collect measurements in both shallow-water (Figure 10) and deep-water environments to capture the range of environmental and submerged conditions on 9 to 14 September. Shallow-water measurements consisted of 164 shallow-water or above-the-water (a diver was not used) measurements (Plymouth: 137 and Buttermilk: 27). Reflectance of various substrates (sand, shell, seagrass, etc.) was measured using the DiveSpec in reflectance mode generating its own illumination. A calibrated white panel was used for reference (E_d) and a calibrated gray panel of 12% reflectance was used throughout data collection to ensure precision in the DiveSpec reflectance measurement. A total of 182 deep-water measurements (Plymouth: 88 and Buttermilk: 94) were taken with the assistance of professional divers from Coastal Diving Services, LLC located in Middletown, RI. Sites were pre-selected based on the results from the acoustic survey for known occurrence of SAV in these regions, as well as other sites representing the other substrate types found in the survey area. DiveSpec measurements were directed and analyzed by Jen Aitken of Optech International.

Figure 10. Operation of the DiveSpec in the shallow-water environment measuring SAV reflectance.

In situ shoreline hyperspectral reflectance measurement. Hyperspectral reflectance measurements were taken with a FieldSpec spectroradiometer (Analytical Spectral Devices, Inc., Boulder, CO) in nearshore sites, including 18 sites in Buttermilk Bay Entrance Channel and 62 sites in Plymouth Harbor on 9 to 14 September. Spectral measurements were taken focusing on targets of interest, such as SAV, marsh grass, macroalgae, and other exposed or emergent vegetation in the nearshore environment. Other targets included large homogenous areas, such as asphalt, sand (dry and wet), bare ground, exposed mudflats, and lawn areas. In addition, a calibrated white panel was measured before measuring target reflectance to ensure accuracy, and spectral measurements were recorded during full sun conditions. Targets were positioned between the instrument and the sun to obtain full illumination and avoid shadow effects. A 12% reflectance calibrated gray panel was measured occasionally to validate reflectance measurements taken with both the FieldSpec and DiveSpec instruments.

Spectral measurements were viewed and saved in "real-time" with a compatible field laptop and the ASD Inc. RS^3 Spectral Acquisition Software, collecting spectra with the 10° field of view (FOV) instrument and saving radiance values for five samples per target measurement (i.e. five samples in a single file). ViewSpec Pro post-processing software was used to import the saved radiance measurements, convert to reflectance, and export as text files and graphed spectral plots, focusing on the 400- to 800-nm spectral range (Figure 11).

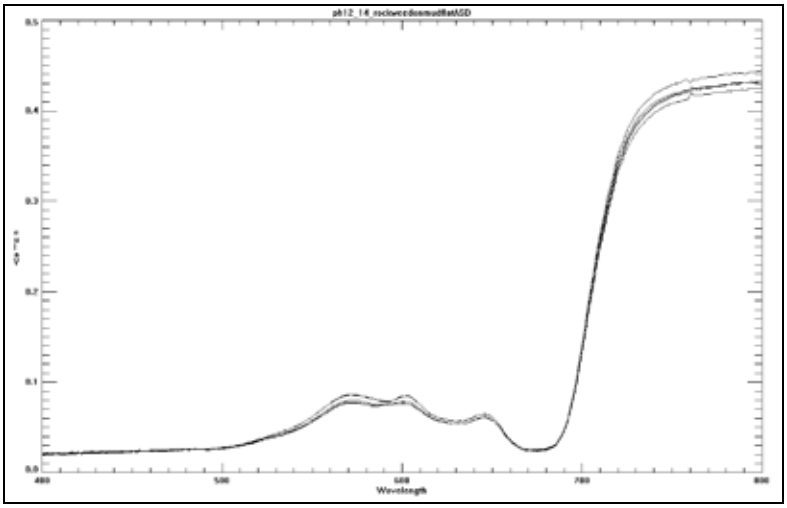

Figure 11. Sample reflectance curves for exposed macroalgae at Plymouth Harbor MA in the 400- to 800-nm spectral range.

These data, along with the measurements from the Divespec, will be used not only for image processing, including the selection of regions of interest to assist with training the classification algorithm and comparison of image and in situ reflectance, but also to assist in verification and accuracy assessment of the final classification results. Shoreline hyperspectral reflectance measurements were collected and analyzed by Molly Reif of ERDC.

Underwater video drop camera. At total of 60 points were selected for each site, 30 based on acoustic survey data and another 30 points selected using Google Earth images, distributed in the survey area outside of the acoustic survey regions. Points were loaded into the NAE survey boat's navigation system for inspection by a video drop camera. A Seaviewer (Seaviewer, Inc., Tampa, FL) low-light underwater video camera system with LED illuminators and onboard control unit was deployed from the survey boat's side winch (Figure 12). Surveys were conducted at Plymouth Harbor on 13 September and at Buttermilk Bay Entrance Channel on 14 September. The survey boat navigated to each pre-planned sampling point and held on station without anchoring. The camera was deployed and video recorded for 10-15 seconds. Following completion of each survey, the video was viewed and bottom conditions were classified with the aid of a pictorial plant guide (Van Patten 2006). GPS position, bottom description, and a grabbed frame were recorded and entered into the database (described later in this technical note). Figure 13 is an

Figure 12. Drop camera, mounted in viewing frame with a 0.5-m x 0.5-m

example of grabbed imagery. Drop camera imagery was collected and interpreted by Richard Loyd, U.S. Army Engineer District, New England.

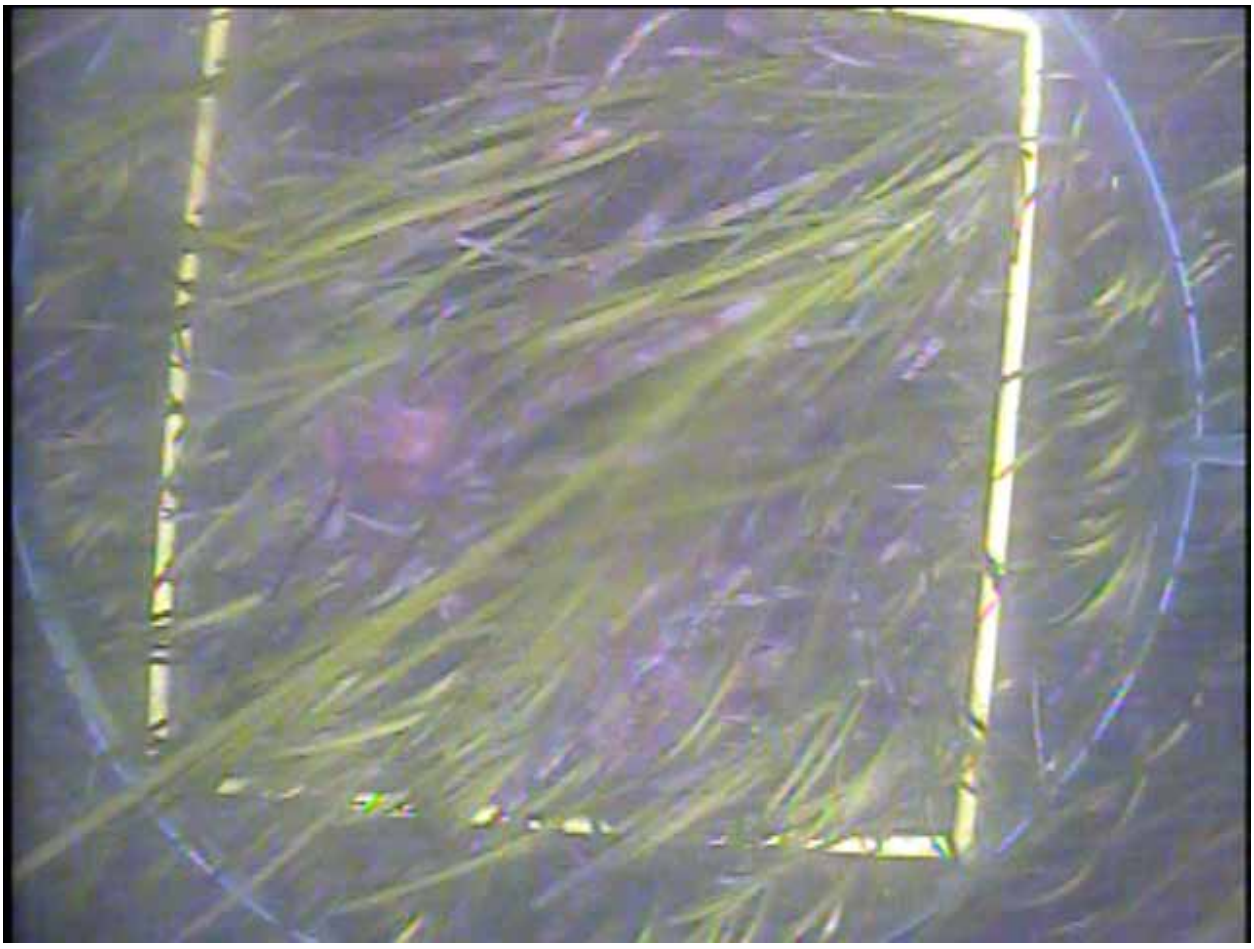

Figure 13. Grabbed video frame (688_PH35) showing eelgrass on sand bottom within 0.5-m quadrant.

Tide measurement. Tidal predictions were retrieved online using software tool XTides 2.0 (http://tbone.biol.sc.edu/tide). The information derived from the software employs an algorithm used by the U. S. National Ocean Service and was used for flight window planning (Figure 4). Tide stations used for the study sites were Plymouth, Cape Cod Bay, MA and Great Hill, Buzzard's Bay, MA.

Real-time tide data were used for the acoustic surveys and were also recorded during the overflight, ranging between 13.9 and 6.9 ft at Plymouth Harbor and between 6.3 and 2.1 ft at Buttermilk Bay Entrance Channel. These measurements were taken to validate predicted tide data, since it is known that predicted tides calculated by the XTides software can deviate by 1 minute or more from official tide readings. During the survey, the water level and time were recorded for every 0.1 ft change in tide. Tide measurements began at least 10 minutes prior to the commencement of the surveys and continued at least 10 minutes post-survey. No permanent tide gage was present at Plymouth Harbor, so a 0.1-ft precision staff gage was affixed to a pier within a sheltered part of the harbor. At Buttermilk Bay Entrance Channel, a permanent tide gage was

located at the USACE Cape Cod Canal office. The tide gage was located on a piling near the Cape Cod Canal docks. While the piling was near the edge of the canal, wave action and boat wake were present and introduced random error into the manual measurements. There was no automated water level gage within Plymouth Harbor. The nearest automated water level gage within Buzzard's Bay was located at Wing's Neck south of the survey area. The tide gage is operated by the USACE Cape Cod Canal office and records water level at 1-minute intervals. The Wing's Neck tide data were electronically transferred to ERDC upon completion of the survey mission. Tide data were collected and compiled by Dr. Candice Piercy, ERDC.

Spectral irradiance. Downwelling irradiance was measured during the overflight on 15 and 16 September at Plymouth Harbor and Buttermilk Bay Entrance Channel using a FieldSpec spectroradiometer (Analytical Spectral Devices, Inc., Boulder, CO). Irradiance values were collected with the Remote Cosine Receptor (180°), which measures irradiance within the geometric hemisphere above the diffuser. Downwelling irradiance was measured at 1-minute intervals during the entire survey period, starting 10 minutes prior to and post survey. Spectral measurements were viewed and saved in "real-time" with the use of a compatible field laptop and the ASD Inc. RS^3 Spectral Acquisition Software. ViewSpec Pro post-processing software was used to import the saved irradiance measurements and export text files. These data will be used for validating atmospheric pre-processing of the hyperspectral imagery. These data were collected by Molly Reif, ERDC.

Diver sampling. Diver sampling consisted of two types of dives – those for rapid observation and those for intensive physical sampling. Acoustic survey data were used to select points for the intensive sampling. Candidate points (15-18) corresponded to high-, medium-, and low-density SAV locations. The goal was to gather nine intensive samples with at least two samples from within each density class. Candidate sampling points (30) for the rapid observation dives were distributed outside of the acoustic sampling area. The target sample size for these dives was 22 per site. The dive team was provided with an excess number of candidate locations, so that locations could be discarded if they were inaccessible at dive time due to tides or if they involved unsafe dive conditions.

Percent cover was measured on the rapid observation dives. Percent cover, shoot density, canopy height, aboveground biomass by species and epiphytic cover were collected and measured at the intensive physical sampling locations. All procedures follow those of Short and Coles (2001). Detailed descriptions of these procedures can be found in Appendix A.

All diving was performed by the U.S Environmental Protection Agency under the direction of Dr. Phil Colarusso. Sampling was conducted at six physical sampling dive locations and 22 rapid observation locations in the Buttermilk Bay Entrance Channel on 14 September and at Plymouth Harbor on 16 September.

Water column optical measurements. Water column optical measurements and water samples were collected at each site during the overflight. Sampling locations were selected throughout the overflight area to coincide with other sampling sites for acoustic, drop camera, and in situ hyperspectral reflectance measurements. Nine locations were sampled at the Buttermilk Bay Entrance Channel site during the 15 September overflight and seven locations were sampled at Plymouth Harbor during the 16 September overflight.

An AC-9 Plus package (WET Labs, Inc., Figure 14) was deployed at each station in a mooring mode, which sampled at a fixed depth of 1-2 m below the sea surface. Salinity and temperature were measured simultaneously using an SBE 19 (Sea-Bird Electronics), which was integrated into the package. The particulate and dissolved absorption and attenuation coefficients, a_{pg} and c_{pg}, were corrected for temperature and salinity (Sullivan et al. 2005) and scattering effects using the proportional correction method (Zaneveld et al. 1994). Drift offsets were obtained from a post-cruise clean-water calibration. Total particulate scattering (b_p) was calculated as the difference between c_{pg} and a_{pg}, assuming that scattering from dissolved material was negligible. The particulate backscattering coefficient (b_{bp}) refers to all the photons that have been redirected in the backward direction due to scattering from particles in the water and to a first order that positively corresponds to the total concentration of particles in the water (reviewed in Stramski et al. (2004)). The backscattering measurements from the WET Labs bbfl2 sensor were corrected for light attenuation effects using concurrent AC-9 data, a chi factor of 0.9 and extrapolated from 90-180° using a third-order polynomial (Sullivan et al. 2005). The Hydroscat backscattering data were processed according to the manufacturer's procedure using a chi factor of 1.08 (Maffione and Dana 1997). Chlorophyll *a* (Chl) was determined from filtered discrete surface water samples fluorometrically and measured in triplicate for each station (Holm-Hansen et al. 1965). Table 2 summarizes these measurements. These data were collected and analyzed by Dr. Heidi Dierssen of the University of Connecticut. A more detailed description of these data may be found in Appendix B.

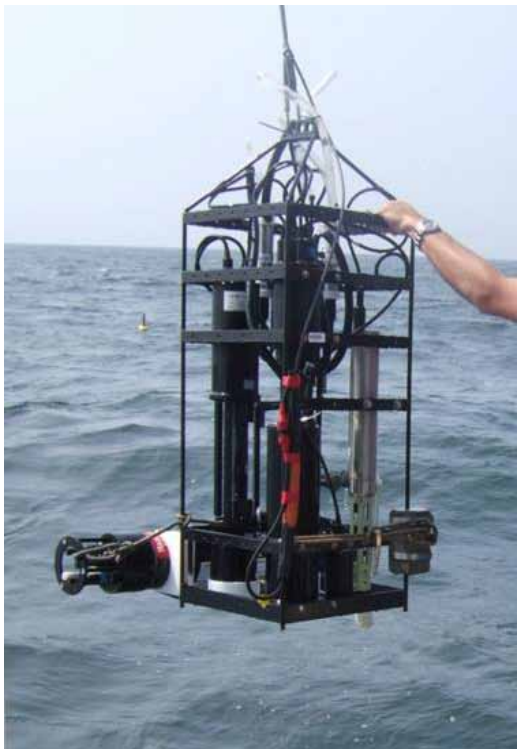

Figure 14. AC-9 Plus instrument package used for optical measurement.

PRELIMINARY CHARTS IMAGERY: Preliminary image and data processing were conducted in the field on 15 and 16 September post survey to assure image acquisition and conduct visual quality assessments. Preliminary processing was conducted with the Optech International Coastal Zone Mapping and Imaging lidar (CZMIL) Data Processing System (DPS), which is an interactive stand-alone software application of the CZMIL system for the creation of information products (Park and Tuell 2010). CZMIL contains six modules spanning the range of processing steps from raw data import to final data product export. Pre-processing of the hyperspectral imagery includes radiometric and atmospheric correction, as well as georeferencing and mosaicking; whereas the lidar point data are imported, georeferenced, and edited in a three-dimensional manual editing environment for the creation of digital elevation models (DEMs).

The pre-processed hyperspectral imagery was inverted using a nonlinear optimization technique (Levenberg-Marquardt algorithm) to solve for seafloor reflectance (Kim et al. 2010). During this process the bathymetric lidar depth was used as a fixed constraint; however, the inversion processing can also be run even if the lidar is not available. Lidar depth, as well as the

Table 2. Water column optical and water quality measurements.		
Instrument	**Measurement**	**Deployment**
ACS and filtered AC9	a_{pg}**([84 spanning 390 to 750 nm]),** particulate+dissolved absorption (m^{-1})	Sampled at fixed 1- to 2-m depth
	a_g**([84 spanning 412 to 715 nm]),** dissolved absorption (m^{-1})	
	a_p**([84 spanning 390 to 750 nm]),** particulate absorption (m^{-1})	
	a_t**([84 spanning 390 to 750 nm]),** total absorption (incl. water) (m^{-1})	
	c_{pg}**([84 spanning 390 to 750 nm]),** particulate+dissolved attenuation (m^{-1})	
	c_p**([84 spanning 390 to 750 nm]),** particulate attenuation coefficient (m^{-1})	
	b_p**([84 spanning 390 to 750 nm]),** particulate scattering (m^{-1})	
BBFL2	b_{bp}**([650 nm]),** particulate backscattering (m^{-1}) b_{bt}**([650 nm]),** total backscattering (incl. water) (m^{-1})	Sampled at fixed 1- to 2-m depth
Hydroscat-6	b_{bp}**([420, 442, 470, 510, 590, and 700 nm]),** particulate backscattering (m^{-1}) b_{bt}**([420, 442, 470, 510, 590, and 700 nm]),** total volume scattering (incl. water) (m^{-1})	Sampled at fixed 1- to 2-m depth
Portable Field-Spec Pro VNIR	**Rrs [derived parameter]**	Measurement made above water.
Chlorophyll	**Extracted Chlorophyll by fluorescence**	Surface samples at selected stations

attenuation coefficient and bottom reflectance at the green channel, which are obtained from the waveform, can be used in the inversion process to reduce parameters and enhance results. Parameters taken from the water column optical measurements were entered into the software during the optimization processing and included chlorophyll, CDOM, and backscattering. The in situ values work to more accurately solve for seafloor reflectance in the Levenberg-Marquardt algorithm. Results of the spectral optimization process include inherent optical properties in the water column estimated for the entire survey area (chlorophyll concentration, DOM absorption, backscattering by particle), bottom reflectance, bottom types, depth (when not used as a provided constraint), water-leaving reflectance, and other output. Comparisons between the spectral optimization output and the other water column optical measurements (i.e. absorption) assist with verifying spectral fitting processes and can be helpful for fine-tuning image processing. Preliminary processing results conducted in DPS are shown in Figures 15 and 16.

During processing, reflectance is compared to spectra in a spectral library and pixels are separated into image grids of various types (i.e. SAV, sand, etc.). The SAV bottom type will be used as a mask on the bottom reflectance to limit the classification and further refinement of the individual species. In addition, variations of the spectral optimization process will be run to test the influence of the lidar depth on the accuracy of the outputs, and ultimately, the classification results. Furthermore, collected in situ spectral and water quality measurements will be used to improve the processing results. Data processing is performed by ERDC and JALBTCX.

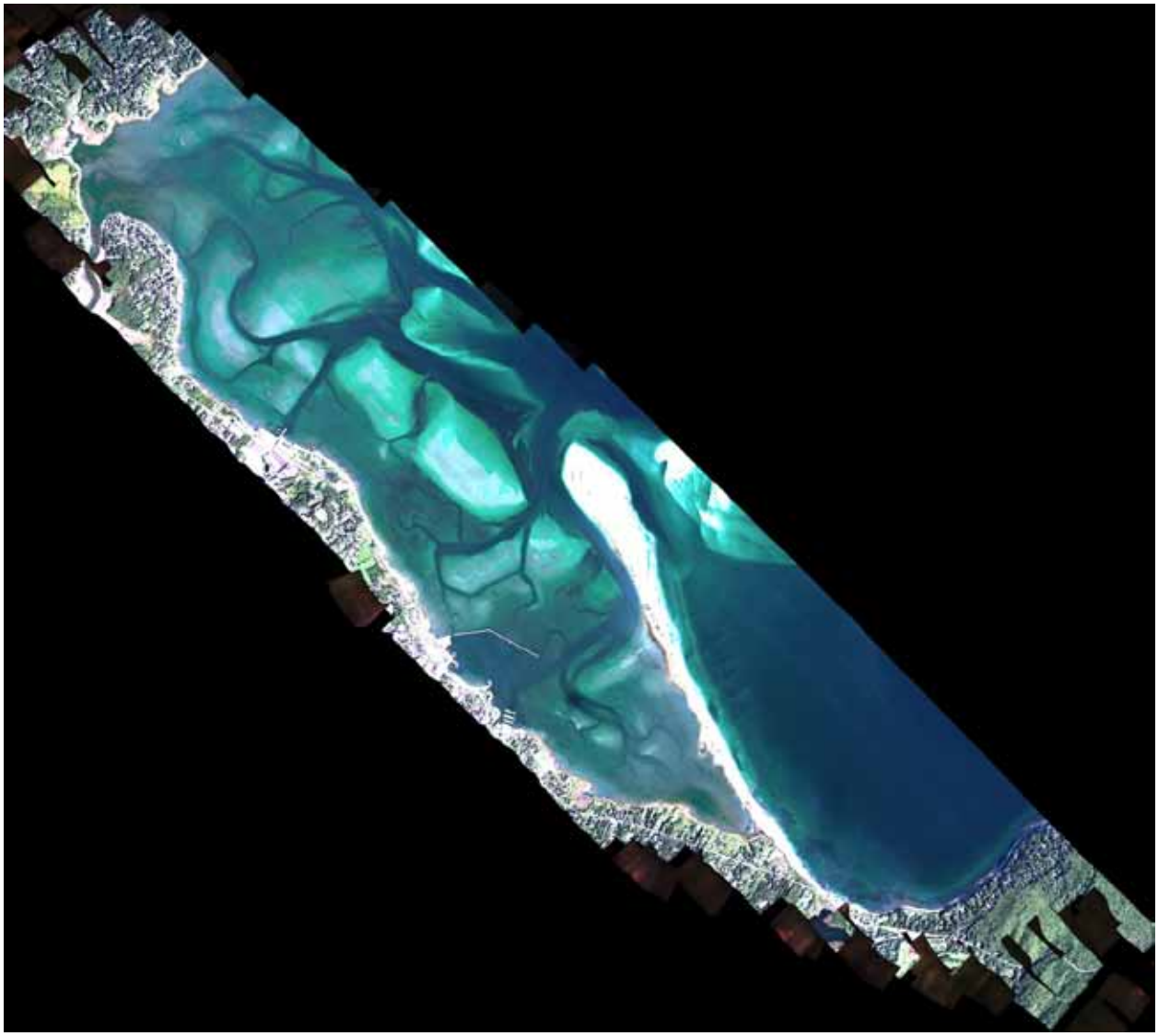

Figure 15. Hyperspectral water-leaving reflectance at Plymouth Harbor as a result of preliminary processing in DPS using spectral optimization. Note the occurrence of channels in deeper blue-green shades, whereas shallow-water areas are represented in lighter blue-green shades. The elongated white feature in the southeast portion of the study is a land spit that is partially submerged during high tide conditions.

DATA MANAGEMENT AND RETRIEVAL: Ground truth data for each site were compiled into a Microsoft Access database. The database contains the complete set of ground truth data for each site including associated text files, imagery, and photos. The ground truth data were compiled into Microsoft Access 2007 and consist of six related tables: Master Table, Percent Cover, Acoustic Transects, Acoustic Points, Biomass, and Optical Properties. Relationships among the database tables are described in Figure 17. The Plymouth Harbor database contains 377 records in the Master Table and the Buttermilk Bay Entrance Channel database contains 237 records in the Master Table.

Figure 16. Elevation/depth at Buttermilk Bay Entrance Channel as a result of preliminary processing in DPS for lidar grid generation. Note that the navigation channel running through the middle section of the image is missing data values because the depths are too great to be detected. Lighter shades represent land, while darker shades represent water, or greater depth values.

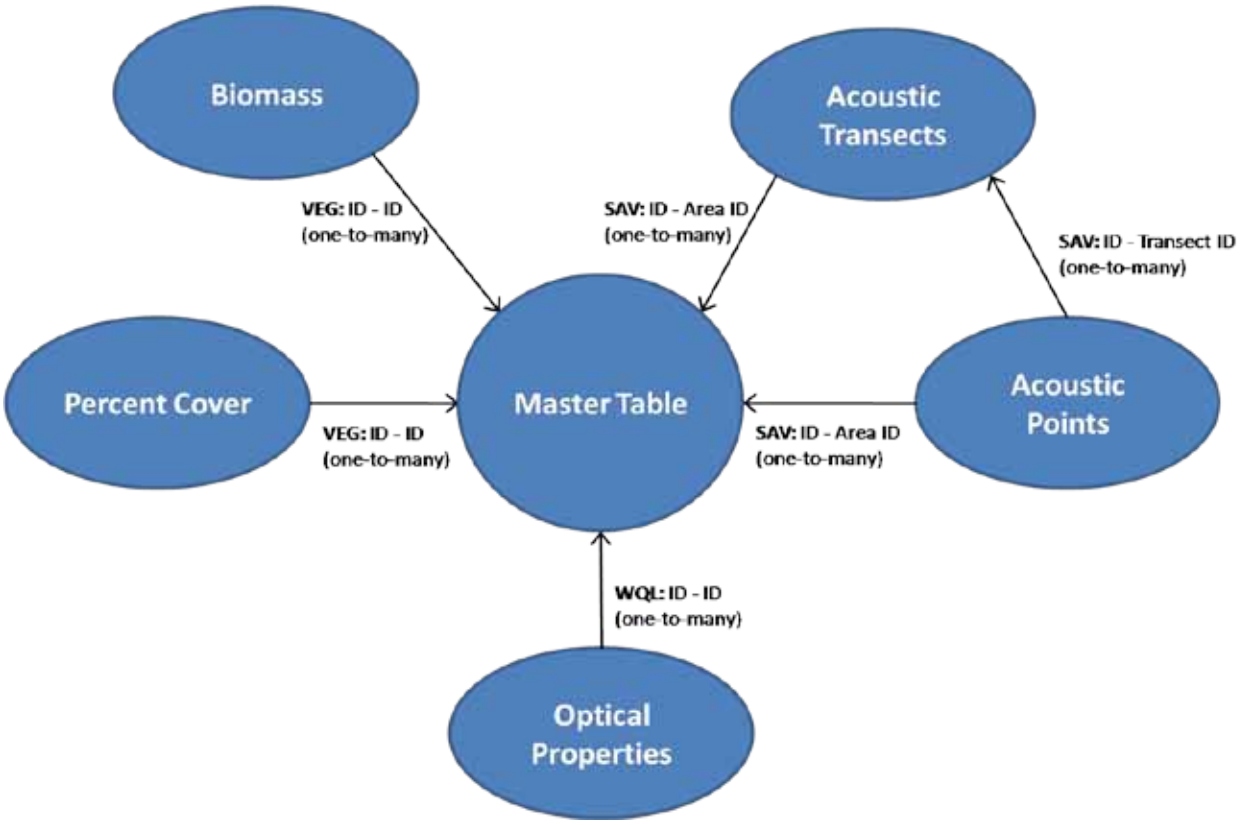

Figure 17. Microsoft Access database table relationships.

The databases contain eight types of data defined in Table 3. All associated data for the ASD, DRC, DVS, and PIC data types are stored in the Master Table. Information for WQL, SAV, and VEG data types are stored in the Master Table and one or more related tables (Table 3). The WQL, SAV, and VEG data types required separate but related tables because the data types required fields that were unique to that data type. The tables were related on the unique ID variable in the Master Table; each unique ID in the Master Table may be related to many records in the related tables. The linked fields are shown in Figure 17. Additional information on the database field definitions can be found in the Readme document packaged with the databases.

The Microsoft Access databases are publically available to interested parties online through the Coastal America website (*http://www.coastalamericafoundation.org*). Coastal America is a partnership between federal agencies including the USACE and the U.S. Environmental Protection Agency, state and local governments, and private organizations dedicated to protecting, preserving, and restoring the nation's coastal ecosystems. Google Earth Keyhole Markup Language-zipped (KMZ) files are also provided on the Coastal America website in addition to the Microsoft Access databases.

The Google Earth KMZ files include some preliminary CHARTS imagery and place markers indicating the locations at which ground truth data were collected for each site (Figure 18). The KMZ contains two folders: the CHARTS folder and the Ground truth data folder. The CHARTS folder contains a rendering of the SHOALS lidar from the 15 and 16 September 2010 airborne surveys, the survey area polygons, and the flight lines. The Ground truth data folder contains

Table 3. Data types stored in the Microsoft Access databases.

Code	Data Type	Stored In:	Number of Entries in Master Table	
			Buttermilk Bay	Plymouth Harbor
ASD	Land-based spectral measurements made with the ASD FieldSpec hand-held spectrometer	Master Table	18	62
DRC	Drop-camera measurements	Master Table	56	52
DVS	Land- and water-based spectral measurements made with the DiveSpec underwater spectrometer	Master Table	121	225
PIC	Land-based picture of unique feature with no other associated measurements	Master Table	2	0
SAV	SAVEWS data	Master Table Acoustic Transects Acoustic Points	3	3
VEG	Diver measurements of vegetation properties	Master Table Biomass Percent Cover	28	28
WQL	In situ chlorophyll and other water optical measurements	Master Table Optical Properties	9	7

Figure 18. Screenshot of Buttermilk Bay Entrance Channel Google Earth KMZ. The green place markers are sites where spectra were collected using the Divespec underwater spectrometer. The red line is the survey area boundary.

place markers indicating the locations where ASD FieldSpec spectrometer, drop camera imagery, Divespec underwater spectrometer, EPA diver vegetation measurements, photographs, and water column optical properties were measured. Each category is color-coded and individually selectable. The place markers are labeled with a brief description of the cover type. The ground truth data folder also contains the acoustic survey area polygons. The database was designed and implemented by Dr. Candice Piercy, ERDC.

ANALYSIS PATH FORWARD: Preliminary processing of the CHARTS data has been conducted, and the remainder of the processing includes refinement of the spectral optimization as well as image classification. An iterative processing and classification plan is described in Table 4. The goals of the CHARTS image processing for detection and discrimination of SAV and macroalgae species are identified, in which both supervised (with training assistance) and unsupervised (no training assistance) classification techniques will be utilized on the bottom reflectance image, resulting from the lidar depth constrained spectral optimization (S/O) output. During the image processing, the hierarchical approach (identified on the vertical axis of Table 4) outlines initial detection of SAV, followed by more rigorous feature identification (discrimination of eelgrass vs. without eelgrass, eelgrass attributes, macroalgae species, and other bottom types). Other analyses include a supervised classification of the hyperspectral water-leaving reflectance (no lidar depth constraint), as well as comparison techniques using or mimicking the settings of other common image formats and SAV detection techniques including: 1) RGB, 20-cm aerial photography for visual photo-interpretation by a local expert, and 2) supervised classification of spectrally and spatially downsampled CASI (to the level of a common multispectral platform, GeoEye-1). These particular analyses have been identified because they represent the current range of (a) processing techniques, such as hyperspectral-only, water-leaving reflectance, aerial photo-interpretation, and spectral optimization, (b) classification approaches, including supervised and unsupervised, (c) feature identification, ranging from SAV detection to macroalgae species identification. These approaches will also illustrate the influence of ground truth on the classification approach, as well as the impact to overall accuracy of detection and species discrimination.

The success and accuracy of remote sensing is largely dependent upon available ground truth and this study illustrates the coordination, collection, and compilation of many types of ground truth data that are critical for effective image processing and accuracy assessment for remote sensing research and development efforts. The detailed activities outlined in this report can also serve as an example and guideline for the types of information, measurement techniques, and use of ground truth in a developmental remote sensing project. The ground truth measurements are useful for deriving more accurate results in the hyperspectral inversion processing (i.e. inherent optical properties in the water column and end member spectra in the spectral library) as well as classification results (i.e. selection of regions of interest), when available. Furthermore, this study is also meant to provide a comprehensive data resource for other scientists working to protect and plan for critical SAV resources and restoration efforts. This document is offered as a case study and no attempt has been made to evaluate this effort or generate any guidance on how best to conduct a ground truth survey for an R&D effort. This evaluation can only be performed after the image analysis has been completed and will be included in the final manuscript at the completion of this project.

Table 4. Image processing and classification plan; cells in table will contain computed classification accuracy metrics based on comparison of classified output with ground truth data.

Priority	Decision Level[1]	Pre-processing Data Groups					
		1) S/O Lidar/CASI (bottom reflectance)	2) S/O Lidar/CASI (bottom reflectance)	3) CASI Only (water-leaving reflectance-wlr)	4) CASI wlr Spectrally Downgraded to GeoEye-I Satellite Spectra	5) RGB 20-cm Aerial Phototography	
1	Detection (SAV/no-SAV						
1	Discrimination (w/ eelgrass vs. w/o eelgrass						
2	Eelgrass attributes						
2	Macroalgae species						
3	Bottom type						
Classification processing		Supervised w/ ground truth (gt) data subset	Unsupervised (no prerequisite gt) (processing on the cheap)	Supervised w/ gt data subset	Supervised w/ gt data subset	Visual interpretation by Charlie Costello (MA DEP)	

[1] All data have been pre-segmented to eliminate land areas.

POINTS OF CONTACT: For additional information, contact Molly Reif (228-252-1134; *Molly.K.Reif@usace.army.mil*) or the manager of the Dredging Operations and Environmental Research (DOER) Program, Dr. Todd Bridges (601-634-3626; *Todd.S.Bridges@usace.army.mil*). This technical note should be cited as follows:

> Reif, M., C. Piercy, J. Jarvis, B. Sabol, C. Macon, R. Loyd, P. Colarusso, H. Dierssen, and J. Aitken. 2012. *Ground truth sampling to support remote sensing research and development: Submersed aquatic vegetation species discrimination using an airborne hyperspectral/lidar system*. DOER Technical Notes Collection. ERDC TN-DOER-E30. Vicksburg, MS: U.S. Army Engineer Research and Development Center.

REFERENCES

Aitken, J.; V. Rammath, V. Feygels, A. Mathur, M. Kim, J. Y. Park, and G. Tuell. 2010. Prelude to CZMIL: Seafloor Imaging and Classification Results Achieved with CHARTS and the Rapid Environmental Assessment (REA) Processor. In *Proceedings of SPIE Algorithms and Technologies for Multispectral, Hyperspectral and Ultraspectral Imagery XVI*, Vol. 7695 (Orlando, FL).

Brando, V.E., and A. G. Dekker. 2003. Satellite hyperspectral remote sensing for estimating estuarine and coastal water quality, IEEE Trans. *IEEE Transactions on Geoscience and Remote Sensing* 41(6): 1378– 1387.

Congalton, R.G. 1988. A comparison of sampling schemes used in generating error matrices for assessing the accuracy of maps generated from remotely sensed data. *Photogrammetric Engineering and Remote Sensing* 54(5): 593–600.

Congalton, R.G., and K. Green. 2009. *Assessing the accuracy of remotely sensed data – Principles and practices.* 2nd ed. Boca Raton, FL: CRC Press, Taylor & Francis Group.

Congalton, R.G., R. G. Oderwald, and R. A. Mead. 1983. Assessing Landsat classification accuracy using discrete multivariate statistical techniques. *Photogrammetric Engineering and Remote Sensing* 49(12): 1671–1678.

Costello, C.T., and W. J. Kenworthy. 2011. Twelve-year mapping and change analysis of eelgrass (*Zostera marina*) areal abundance in Massachusetts (USA) identifies statewide declines. *Estuaries and Coasts* 34(2): 232-242.

Dekker, A.G., V. E. Brando, J. M. Anstee, S. Fyfe, T.J.M. Malthus, and E. Karpouzli. 2006. Remote sensing of seagrass ecosystems: Use of spaceborne and airborne sensors. In *Biology of seagrasses: Biology, Ecology and Conservation*, ed. A.W.D. Larkum, C.M. Duarte, and R.J. Orth. Springer: 347-359.

Dennison, W.C., R.J. Orth, K.A. Moore, J.C. Stevenson, V. Carter, S. Kollar, P.A. Bergstrom, and R.A. Batiuk. 1993. Assessing water quality with submersed aquatic vegetation: Habitat requirements as barometers of Chesapeake Bay health. *BioScience* 43(2): 86–94.

Duffy, K.C., and D. M. Baltz. 1998. Comparison of fish assemblages associated with native and exotic submerged macrophytes in the Lake Pontchartrain estuary, U.S.A. *Journal of Experimental Marine Biology and Ecology* 223: 199–221.

Fitzpatrick-Lins, K. 1981. Comparison of sampling procedures and data analysis for a landuse and land-cover map. *Photogrammetric Engineering and Remote Sensing* 47(3): 343–351.

Fonseca, M.S., and J. A. Cahalan. 1992. A preliminary evaluation of wave attenuation by four species of seagrass. *Estuary Coastal Shelf Science* 35: 565–576.

Ginevan, M.E. 1979. Testing land-use map accuracy: Another look. *Photogrammetric Engineering and Remote Sensing* 45(10): 1371–1377.

Hay, A.M. 1979. Sampling designs to test land-use map accuracy. *Photogrammetric Engineering and Remote Sensing* 45(4): 529–533.

Holm-Hansen, O., C. Lorenzen, R. Holmes, and J. Strickland. 1965. Fluorometric determination of chlorophyll, ICES. *Journal of Marine Science* 30(1): 3-15.

Hord, R.M., and W. Brooner. 1976. Land-use map accuracy criteria. *Photogrammetric Engineering and Remote Sensing* 42(5): 671–677.

Kemp, W.M., W.R. Boynton, J.E. Adolf, D. F. Boesch, W.C. Boicourt, G. Brush, J.C. Cornwell, T.R. Fisher, P.M. Glibert, J.D. Hagy, L.W. Harding, E.D. Houde, D.G. Kimmel, W.D. Miller, R.I.E. Newell, M.R. Roman, E.M. Smith, and J.C. Stevenson. 2005. Eutrophication of Chesapeake Bay: Historical trends and ecological interactions. *Marine Ecology Progress Series* 303: 1-29.

Kim, M., J.Y. Park, and G. Tuell. 2010. A constrained optimization technique for estimating environmental parameters from CZMIL Hyperspectral and lidar Data. In *Proceedings of SPIE Algorithms and Technologies for Multispectral, Hyperspectral and Ultraspectral Imagery XVI*, Vol. 7695 (Orlando, FL).

Lillesand, T.M., R.W. Kiefer, and J. W. Chipman. 2004. *Remote sensing and image interpretation*. 5th ed. Hoboken, NJ: John Wiley & Sons.

Maffione, R.A., and D. R. Dana. 1997. Instruments and methods for measuring the backward scattering coefficient of oceanic waters. *Applied Optics* 36: 6057-6067.

McKenzie, L. J., M.A. Finkbeiner, and H. Kirkman. 2001. Methods for mapping seagrass distribution. In *Global seagrass research methods*, ed. F.T. Short and R.G. Coles. Elsevier Press.

Moore, K.A. 2004. Influence of seagrasses on water quality in shallow regions of the lower Chesapeake Bay. *Journal of Coastal Research* 81: 162-178.

Orth, R.J., T.J.B. Carruthers, W.C. Dennison, C.M. Duarte, J.W. Fourqurean, K.L. Heck, Jr., A.R. Hughes, G.A. Kendrick, W.J. Kenworthy, S. Olyarnik, F.T. Short.F.T., M. Waycott, and S.L. Williams. 2006. A global crisis for seagrass ecosystems. *BioScience* 56(12): 987-996.

Park, J.Y., and G. Tuell. 2010. Conceptual design of the CZMIL data processing system (DPS): Algorithms and software for fusing lidar, hyperspectral data, and digital images. In *Proceedings of SPIE Algorithms and Technologies for Multispectral, Hyperspectral and Ultraspectral Imagery XVI*, Vol. 7695 (Orlando, FL).

Phinn, S., C. Roelfsema, A. Dekker, V. Brando, and J. Anstee. 2008. Mapping seagrass species, cover and biomass in shallow waters: An assessment of satellite multispectral and airborne hyper-spectral imaging systems in Moreton Bay (Australia). *Remote Sensing of Environment* 112(8): 3413–3425.

Pinnel, N., T. Heege, and S. Zimmermman. 2004. Spectral discrimination of submerged macrophytes in lakes using hyperspectral remote sensing data. In *SPIE Proceedings on Ocean Optics XVII* 1:1–16.

Richardson, W.B., S.J. Zigler, and M.R. Dewey. 1998. Bioenergetic relations in submerged aquatic vegetation: An experimental test of prey use by juvenile bluegills. *Ecology of Freshwater Fish* 7:1-12.

Rosenfield, G.H., K. Fitzpatrick-Lins, and H. Ling. 1982. Sampling for thematic map accuracy testing. *Photogrammetric Engineering and Remote Sensing* 48(1): 131–137.

Sabol, B., D. Shafer, and E. Lord. 2005. Dredging effects on eelgrass in a New England small boat harbor. *Journal of Marine Environmental Engineering* 8: 57-81.

Sabol, B., E. Lord, K. Reine, and D. Shafer. 2008. *Comparison of acoustic and aerial photographic methods for quantifying the distribution of submersed aquatic vegetation in Sagamore Creek, NH*. DOER Technical Notes Collection. ERDC TN-DOER-E23. Vicksburg, MS: U. S. Army Engineer Research and Development Center.

Sabol, B., R.E. Melton,R. Chamberlain,P. Doering,and K. Haunert. 2002. Evaluation of a digital echo sounder for detection of submersed aquatic vegetation. *Estuaries* 25(1):133-141.

Sabol, B.M., J. Kannenberg, and J.G. Skogerboe. 2009. Integrating acoustic mapping into operational aquatic plant management: A case study in Wisconsin. *Journal of Aquatic Plant Management* 47: 44-52.

Short, F.T., and R.G. Coles (eds.). 2001. *Global seagrass research methods*. Amsterdam: Elsevier Science B.V.

Silva, T.S.F., M.P.F. Coasta, J.M. Melack, and E.M.L.M. Novo. 2008. Remote sensing of aquatic vegetation: Theory and applications. *Environmental Monitoring and Assessment* 140(1-3):131-145.

Sprenkle, E.S., L.A. Smock, and J.E. Anderson. 2004. Distribution and growth of submerged aquatic vegetation in the Piedmont section of the James River, Virginia. *Southeastern Naturalist 3*(3): 517–530.

Stehman, S. 1992. Comparison of systematic and random sampling for estimating the accuracy of maps generated from remotely sensed data. *Photogrammetric Engineering and Remote Sensing* 58(9): 1343–1350.

Stramski, D., E. Boss, D. Bogucki, and K.J. Voss. 2004. The role of seawater constituents in light backscattering in the ocean. *Progress in Oceanography* 61: 27-56.

Sullivan, J., M. Twardowski, P. Donaghay, and S. Freeman. 2005. Use of optical scattering to discriminate particle types in coastal waters. *Applied Optics* 44(9): 1667–1680, doi:10.1364/AO.44.001667.

Tamaki, H., M. Tokuoka, W. Nishijima, T. Terawaki, and M. Okada. 2002. Deterioration of eelgrass, *Zostera marina* L., meadows by water pollution in Seto Inland Sea, Japan. *Marine Pollution Bulletin* 44: 1253 – 1258.

Thorhaug, A., A.D. Richardson, and G.P. Berlyn. 2007. Spectral reflectance of the seagrasses: *Thalassia testudinum, Halodule wrightii, Syringodium filiforme* and five marine algae. *International Journal of Remote Sensing* 28(7): 1487-1501.

U.S. Army Corps of Engineers (USACE), New England District. 2005. *Environmental assessment and finding of No Significant Impact for maintenance dredging and disposal: Plymouth Harbor, Plymouth, Massachusetts*.

van Genderen, J.L., and B.F. Lock.1977. Testing land use map accuracy. *Photogrammetric Engineering and Remote Sensing* 43(9): 1135–1137.

Van Patten, M.S. 2006. *Seaweeds of Long Island Sound*. Groton, CT: Connecticut Seagrant Program.

Wang, Y., M. Traber, B. Milstead, and S. Stevens. 2007. Terrestrial and submerged aquatic vegetation mapping in Fire Island National Seashore using high spatial resolution remote sensing data. *Marine Geodesy* 30(1): 77−95.

Williams, D.J., N. B. Rybicki, A.V. Lombana, T.M. O'Brien, and R.B. Gomez. 2003. Preliminary investigation of submerged aquatic vegetation mapping using hyperspectral remote sensing. *Environmental Monitoring and Assessment* 81(1): 383-392.

Wolter, P.T., C.A. Johnston, and G.J. Niemi. 2005. Mapping submergent aquatic vegetation in the US Great lakes using Quickbird satellite data. *International Journal of Remote Sensing* 26(23): 5255−5274.

Wozencraft, J.M., and W.J. Lillycrop. 2006. JALBTCX coastal mapping for the USACE. *International Hydrographic Review* 7(2): 28-37.

Yuan, L., and L. Zhang. 2008. Mapping large-scale distribution of submerged aquatic vegetation coverage using remote sensing. *Ecological Informatics* 3(3): 245-251.

Zaneveld, J.R.V., J.C. Kitchen, and C.C. Moore.1994. Scattering error correction of reflecting-tube absorption meters. In *Proceedings of Ocean Optics XII*, ed. S.J. Jaffe. SPIE Ocean Optics XII 2258: 44–55.

Zimmerman, R.C., and A.G. Dekker. 2006. Aquatic optics: Basic concepts for understanding how light affects seagrasses and makes them measurable from space. In *Biology of seagrasses: Biology, ecology and conservation*, ed. A. W.D. Larkum, C.M. Duarte, and R.J. Orth. Springer:295-301.

Appendix A: Planning Document

To obtain the planning document for this research, please contact:

Molly Reif
U.S. Army Engineer Research and Development Center
Joint Airborne Lidar Bathymetry Technical Center of eXpertise
7225 Stennis Airport Road, Suite 100
Kiln, MS 39556
228-252-1134
Molly.K.Reif@usace.army.mil

Bruce Sabol
U.S. Army Engineer Research and Development Center
3909 Halls Ferry Road
Vicksburg, MS 39180-6199
601-634-2297
Bruce.M.Sabol@usace.army.mil

Appendix B: Technical Report

To obtain a technical report that is a companion to this research, please contact:

Molly Reif
U.S. Army Engineer Research and Development Center
Joint Airborne Lidar Bathymetry Technical Center of eXpertise
7225 Stennis Airport Road, Suite 100
Kiln, MS 39556
228-252-1134
Molly.K.Reif@usace.army.mil

Bruce Sabol
U.S. Army Engineer Research and Development Center
3909 Halls Ferry Road
Vicksburg, MS 39180-6199
601-634-2297
Bruce.M.Sabol@usace.army.mil

Appendix C: Background Documents

To obtain additional background documents relevant to the research described in this technical note, please contact:

Molly Reif
U.S. Army Engineer Research and Development Center
Joint Airborne Lidar Bathymetry Technical Center of eXpertise
7225 Stennis Airport Road, Suite 100
Kiln, MS 39556
228-252-1134
Molly.K.Reif@usace.army.mil

Bruce Sabol
U.S. Army Engineer Research and Development Center
3909 Halls Ferry Road
Vicksburg, MS 39180-6199
601-634-2297
Bruce.M.Sabol@usace.army.mil